



Vaccine Adjuvants

Take your vaccine to the next level

InVivoGen



***Tupaia* GBP1 Interacts with STING to Initiate Autophagy and Restrict Herpes Simplex Virus Type 1 Infection**

This information is current as of December 4, 2021.

Tianle Gu, Dandan Yu, Ling Xu, Yu-Lin Yao and Yong-Gang Yao

J Immunol 2021; 207:2673-2680; Prepublished online 3 November 2021;

doi: 10.4049/jimmunol.2100325

<http://www.jimmunol.org/content/207/11/2673>

Supplementary Material <http://www.jimmunol.org/content/suppl/2021/11/03/jimmunol.2100325.DCSupplemental>

References This article **cites 54 articles**, 15 of which you can access for free at: <http://www.jimmunol.org/content/207/11/2673.full#ref-list-1>

Why *The JI*? Submit online.

- **Rapid Reviews! 30 days*** from submission to initial decision
- **No Triage!** Every submission reviewed by practicing scientists
- **Fast Publication!** 4 weeks from acceptance to publication

**average*

Subscription Information about subscribing to *The Journal of Immunology* is online at: <http://jimmunol.org/subscription>

Permissions Submit copyright permission requests at: <http://www.aai.org/About/Publications/JI/copyright.html>

Email Alerts Receive free email-alerts when new articles cite this article. Sign up at: <http://jimmunol.org/alerts>



Tupaia GBP1 Interacts with STING to Initiate Autophagy and Restrict Herpes Simplex Virus Type 1 Infection

Tianle Gu,^{*,†,‡} Dandan Yu,^{*,§,¶,||} Ling Xu,^{*,§,¶,||} Yu-Lin Yao,^{*,‡} and Yong-Gang Yao^{*,‡,§,¶,||}

Stimulator of IFN genes (STING) is a key molecule that binds to cyclic dinucleotides produced by the cyclic GMP-AMP synthase to activate IFN expression and autophagy in the fight against microbial infection. The regulation of STING in the activation of IFN expression has been extensively reported, whereas the regulation of STING in the initiation of autophagy is still insufficiently determined. IFN-inducible guanylate-binding proteins (GBPs) are central to the cell-autonomous immunity in defending a host against viral, bacterial, and protozoan infections. In this study using the Chinese tree shrew (*Tupaia belangeri chinensis*), which is genetically close to primates, we found that *Tupaia* GBP1 (tGBP1) combines with *Tupaia* STING (tSTING), promotes autophagy, and moderately inhibits HSV type 1 (HSV-1) infection. The antiviral effects of tGBP1 are IFN independent. Mechanistically, tGBP1 interacted with tSTING, *Tupaia* sequestosome 1, and *Tupaia* microtubule associated protein 1 L chain 3, forming a complex which promotes autophagy in response to HSV-1 infection. This function of tGBP1 against HSV-1 infection was lost in tSTING knockout cells. Overexpression of either tSTING or its mutant tSTING-ΔCTT that can only activate autophagy rescued the anti-HSV-1 activity of tGBP1 in tSTING knockout cells. Our study not only elucidated the underlying mechanism of tGBP1 antiviral activity against HSV-1 infection, but also uncovered the regulation of tSTING in the initiation of autophagy in response to HSV-1 infection. *The Journal of Immunology*, 2021, 207: 2673–2680.

The innate immune response provides a host with a robust first line of defense against viral infections (1). This relies on pattern recognition receptors to detect viral invasion, which in turn leads to the production of type I IFNs (2). Cytoplasmic RNAs derived from the viral genome or its replication intermediates are mainly recognized by retinoic acid inducible gene I (RIG-I)-like receptors including RIG-I, melanoma differentiation-associated protein 5 (MDA5), and laboratory of genetics and physiology 2 (3). The appearance of pathogen-derived DNA (such as viral DNA) or self-DNA from genomic DNA damage in the cytoplasm of mammalian cells is detected by the enzyme cyclic GMP-AMP synthase (cGAS) that catalyzes the formation of 2',3'-cyclic GMP-AMP (cGAMP) (4). cGAMP functions as a second messenger that directly binds to the endoplasmic reticulum (ER)-anchored adaptor protein stimulator of IFN genes (STING) for activation. The activated STING then moves from the ER to the ER-Golgi intermediate compartments and the Golgi apparatus (5, 6), where it recruits TANK-binding kinase 1 and IFN regulatory factor 3 by C-terminal tail (CTT) domain, leading to the production of type I IFNs (7, 8). Meanwhile, STING-containing ER-Golgi intermediate compartments serve as a membrane source for microtubule-associated protein 1 L chain 3 (LC3) lipidation and STING binds to sequestosome

1 (SQSTM1) or LC3 to initiate autophagy, which is important for the clearance of DNA and viruses in the cytosol (9, 10). STING in *Nematostella vectensis* does not contain the CTT domain, which resembles STING-ΔCTT, and maintains the ability to induce autophagy but not IFNs in response to cGAMP, suggesting that autophagy induction is STING's primordial function (10). The mechanism and regulation of STING in inducing the expression of IFNs have been extensively reported (11), whereas the regulation of STING in activating autophagy is still not sufficiently determined in different species.

Guanylate-binding protein (GBP)1 belongs to the GBP family, which is induced by IFNs and many other inflammatory cytokines such as TNF- α and IL-1 β (12–15). These proteins share a common domain architecture consisting of a globular N-terminal GTPase domain and a C-terminal helical domain (CTD) that allow protein–protein or protein–lipid interactions (16). GBP1 has been shown to be an important mediator of host defense against bacterial pathogens and parasites via oligomerization on pathogen-containing membrane-bound compartments and prompting an array of antimicrobial activities (17), including the production of radical oxygen species by corecruited oxidases (18), the fusion of pathogen-containing membrane-bound

*Key Laboratory of Animal Models and Human Disease Mechanisms of the Chinese Academy of Sciences & Yunnan Province, Kunming Institute of Zoology, Kunming, China; [†]College of Life Science, Yan'an University, Yan'an, China; [‡]Kunming College of Life Science, University of Chinese Academy of Sciences, Kunming, China; [§]KIZ-CUHK Joint Laboratory of Bioresources and Molecular Research in Common Diseases, Kunming Institute of Zoology, Chinese Academy of Sciences, Kunming, China; [¶]National Resource Center for Non-Human Primates, Kunming Institute of Zoology, Chinese Academy of Sciences, Kunming, China; and ^{||}National Research Facility for Phenotypic and Genetic Analysis of Model Animals (Primate Facility), Kunming Institute of Zoology, Chinese Academy of Sciences, Kunming, China

ORCID: 0000-0002-2955-0693 (Y.-G.Y.).

Received for publication April 8, 2021. Accepted for publication September 27, 2021.

This work was supported by grants from the National Natural Science Foundation of China (U1902215 to Y.-G.Y.), the People's Government of Yunnan Province (202001AS070023 to D.Y.) and the Chinese Academy of Sciences Light of West China Program (xbzg-zdsys-201909 to Y.-G.Y.).

Address correspondence and reprint requests to Dr. Yong-Gang Yao, Kunming Institute of Zoology, Chinese Academy of Sciences, Kunming, Yunnan 650204, China. E-mail address: yaoyg@mail.kiz.ac.cn

The online version of this article contains supplemental material.

Abbreviations used in this article: CBD, cyclic GAMP-binding domain; cGAMP, 2', 3'-cyclic GMP-AMP; cGAS, cyclic GMP-AMP synthase; CTD, C-terminal helical domain; CTT, C-terminal tail; ER, endoplasmic reticulum; GBP, guanylate-binding protein; HSV-1, HSV type 1; KSHV, Kaposi's sarcoma-associated herpesvirus; LC3, microtubule-associated protein 1 L chain 3; MDA5, melanoma differentiation-associated protein 5; MOI, multiplicity of infection; SQSTM1, sequestosome 1; STING, stimulator of IFN genes; tGBP1, *Tupaia* GBP1; tLC3, *Tupaia* LC3; TM, transmembrane; tMAVS, *Tupaia* mitochondrial antiviral signaling protein; tMDA5, *Tupaia* MDA5; tSQSTM1, *Tupaia* SQSTM1; tSTING, *Tupaia* STING; TSPRC, tree shrew primary renal cell; TSR, tree shrew renal; VSV, vesicular stomatitis virus.

Copyright © 2021 by The American Association of Immunologists, Inc. 0022-1767/21/\$37.50

compartments with degradative lysosomes (19), their encapsulation within autophagosome-like structures (20), and the lytic disintegration of microbe-containing compartments (21, 22). Most recently, GBP1 was reported to act as a cytosolic LPS sensor and assemble a platform for caspase-4 recruitment and activation at LPS-containing membranes as the first step of non-canonical inflammasome signaling in human epithelial cells (23). GBP1 is also involved in the host innate immune response to viral infections (17). Overexpression of GBP1 inhibits the replication of the vesicular stomatitis virus (VSV) (24, 25), the encephalomyocarditis virus (24), the hepatitis C virus (26), the Kaposi's sarcoma-associated herpesvirus (KSHV) (27), and the classical swine fever virus (28). Although the antiviral function of GBP1 to KSHV infection was reported to involve the disruption of the F-actin-formed cytoskeleton, the mechanism of the antiviral activity of GBP1 against the other viruses has not been sufficiently examined (28).

We have previously identified five *GBP* genes (*tGBP1*, *tGBP2*, *tGBP4*, *tGBP5*, and *tGBP7*) in the Chinese tree shrew (29), a small mammal genetically close to primates (30, 31), which has proved to be a particularly good model for the study of infectious diseases (32–36) and other diseases (37, 38). By using this model, we found that *Tupaia* GBP1 (*tGBP1*) can control the infection of VSV and HSV type 1 (HSV-1) in tree shrew primary renal cells (TSPRCs) (29). We also demonstrated that *tGBP1* exerts an anti-VSV function by competing with the VSV nucleocapsid protein in binding to the VSV phosphoprotein, leading to repression of the primary transcription of the VSV genome (25). However, the mechanism of antiviral function of *tGBP1* in response to HSV-1 infection remained unclear.

Here, we report the underlying mechanism of *tGBP1* antiviral activity against HSV-1 infection. We identified *tGBP1* as an important mediator for *Tupaia* STING (*tSTING*) to induce autophagy in response to HSV-1 infection. However, unlike the human form of STING which interacts directly with SQSTM1 and LC3 to initiate autophagy (9, 39), *tSTING* does not bind to *Tupaia* SQSTM1 (*tSQSTM1*) or *Tupaia* LC3 (*tLC3*). Instead, *tGBP1* interacts with *tSTING*, *tSQSTM1*, and *tLC3* to act as a scaffold for *tSTING*, *tSQSTM1*, and *tLC3* interaction and promote autophagy in response to HSV-1 infection.

Materials and Methods

Experimental animals and cells

The Chinese tree shrews were purchased from the experimental animal core facility of Kunming Institute of Zoology, Chinese Academy of Sciences. After euthanasia, TSPRCs were isolated from tree shrew renal (TSR) tissue according to the method of enzyme assisted dissection, as described in our previous study (40, 41). This study was approved by the Institutional Animal Care and Use Committee of Kunming Institute of Zoology.

The TSR cell line (TSR6) was established in our previous study (42). It was immortalized from TSPRCs by using SV40 large T Ag transduction (42). TSR6 cells with *tGBP1* knockout (TSR6-*tGBP1*-KO (29)) and *tSTING* knockout (TSR6-*tSTING*-KO (43)) were established in our previous studies using the CRISPR/Cas9 gene editing method (44). HEK293T cells were obtained from the Kunming Cell Bank, Kunming Institute of Zoology. Cells were cultured at 37°C in 5% CO₂ with DMEM (11965-092; Life Technologies-BRL) supplemented with 10% FBS (10099-141; Life Technologies-BRL) and 1 × penicillin/streptomycin (10378016; Life Technologies-BRL).

Reagents, Abs, and plasmids

Restriction enzymes *Bam*HI, *Xho* I, and T4 DNA ligase (Thermo Fisher Scientific) were used in this study. We used the following Abs: mouse monoclonal anti-Flag (M20008; Abmart), mouse monoclonal anti-β-actin (E1C602-2; EnoGene), mouse monoclonal anti-Myc (MA1-21316-1MG; Invitrogen), rabbit monoclonal anti-Myc (18583; Cell Signaling Technology), rabbit monoclonal anti-SQSTM1/P62 (8025T; Cell Signaling Technology), rabbit monoclonal anti-LC3B (3868S; Cell Signaling Technology), mouse

monoclonal anti-GBP1 (67161-1-Ig; proteintech) and rabbit monoclonal anti-STING (13647; Cell Signaling Technology).

Expression vectors for *Tupaia* MDA5 (*tMDA5*) (pCMV-HA-*tMDA5*) (45), *Tupaia* mitochondrial antiviral signaling protein (*tMAVS*) (pCMV-HA-*tMAVS*) (45), *tSTING* (pCS-Myc-*tSTING*) (43), and *tGBP1* (pCMV-*tGBP1*-3Tag-8) (29) were constructed in our previous studies. We created two plasmids encoding truncated *tGBP1* mutants, *tGBP1*-GTPase (pCMV-*tGBP1*-GTPase-3Tag-8) and *tGBP1*-CTD (pCMV-*tGBP1*-CTD-3Tag-8), by subcloning from the pCMV-*tGBP1*-3Tag-8. The pCMV-3Tag-8 expression vector for *tSTING* and pCS-Myc-N expression vectors for different *tSTING* domains (*tSTING*-transmembrane [TM] [pCS-Myc-N-*tSTING*-TM], *tSTING*-cyclic GAMP-binding domain [CBD] [pCS-Myc-N-*tSTING*-CBD], and *tSTING*-ΔCTT [pCS-Myc-N-*tSTING*-ΔCTT]) were subcloned from pCS-Myc-*tSTING*. The pCS-Myc-N expression vector for *tMDA5* was subcloned from pCMV-HA-*tMDA5*. The *tSQSTM1* (pCS-Myc-N-*tSQSTM1*) and *tLC3B* (pCS-Myc-N-*tLC3B*) constructs were generated using gene-specific primer pairs and were cloned into pCS2-N-Myc vector. Primers used in this study are listed in Supplemental Table I. All constructs were verified by sequencing.

Viral infection

HSV-1 strain 17+ (simplified to just HSV-1) was amplified as in our previous studies (29, 43). HSV-1 with a GFP tag (HSV-1-GFP) was obtained from Prof. Jumin Zhou's laboratory at Kunming Institute of Zoology. For viral infection, cells seeded in a 24-well (5 × 10⁴ per well) or 6-well plate (2 × 10⁵ per well) were washed three times with PBS (pH 7.4), incubated with HSV-1 or HSV-1-GFP (multiplicity of infection [MOI] = 1) for 1 h in DMEM without FBS, and then rinsed and cultured in fresh growth medium containing 1% FBS until harvest.

RNA isolation and quantitative RT-PCR

Total RNA was extracted by using RNAsimple Total RNA Kit (DP419; Tiangen) according to the manufacturer's instructions. The cDNA was synthesized by using M-MLV reverse transcriptase with random primer (M1701; Promega). Quantitative RT-PCR was performed using iTaq Universal SYBR Green Supermix (1725124; Bio-Rad, USA) supplemented with gene-specific primers (Supplemental Table I) on a CFX Connect Real-Time System (Bio-Rad), as described in our previous studies (41, 46). We serially diluted the PCR product to achieve the 10⁻³–10⁻¹⁰ dilutions for generating the standard curves. Ct values were measured with the respective standard curves. The tree shrew housekeeping gene β-actin was used as the reference gene for normalization.

Transfection, luciferase reporter assay, immunoprecipitation, and Western blotting

TSPRCs and TSR6 cells were transfected with Lipo3000 (L300015; Thermo Fisher Scientific), and HEK293T cells were transfected with X-tremeGENE HP (Roche, 06366546001) according to the manufacturer's instructions.

For luciferase reporter assay, TSPRCs were seeded in a 24-well plate and cultured overnight. Cells were transiently transfected with 100 ng of the luciferase reporter vector (ISRE-Luc and NF-κB-Luc that were reported in our previous studies (41)) and 10 ng pRL-SV40-Renilla, together with 400 ng expression vector (empty vector, vector; pCMV-*tGBP1*-3Tag-8, *tGBP1*; pCS-Myc-*tSTING*, *tSTING*). Cells were harvested at 24 h posttransfection for measuring luciferase activity using the Dual-Luciferase Reporter Assay System (E1960; Promega) on a Luminoskan Ascent instrument (Thermo Fisher Scientific).

For Western blotting, cells were lysed with RIPA lysis buffer (P0013; Beyotime) on ice and centrifuged at 12,000 × g for 10 min at 4°C to remove cell debris. The protein concentration was determined using the BCA protein assay kit (P0012; Beyotime). A total of 20 μg protein was separated with a 12% or 15% (vol/vol) SDS-polyacrylamide gel and electrophoretically transferred onto a polyvinylidene difluoride membrane (L1620177; Bio-Rad). Membranes were blocked with 5% (wt/vol) BSA in TBS supplemented with 0.1% Tween 20 (TBST) (#9997; Cell Signaling Technology) for 2 h at room temperature, then were incubated with respective primary Ab against Myc (1:5000), Flag (1:5000), SQSTM1 (1:1000), LC3B (1:1000), or β-actin (1:10,000) overnight at 4°C. After three washes with TBST (each 5 min), the membranes were incubated for 1 h with anti-mouse or anti-rabbit secondary Ab (1:10,000; KPL, USA; depends on the first Ab) at room temperature. The epitope was visualized by using an ECL Western blotting detection kit (WBKLS0500; Millipore).

For immunoprecipitation, appropriate Abs were incubated with protein G agarose beads (15920010; Life Technologies) to form a complex for 2 h at room temperature. Cells were lysed with RIPA lysis buffer on ice for 1 h, followed by a centrifugation at 12,000 × g for 10 min at 4°C. Five percent of the cell lysate was taken as the input, and the remaining lysate was incubated with the Ab protein G (10004D; Invitrogen) beads complex overnight

at 4°C. After four washes with RIPA lysis buffer, the immunoprecipitants were separated by SDS-PAGE and analyzed by immunoblotting.

Immunofluorescence

TSPRCs were seeded in a chamber slide (154526; Thermo Fisher Scientific) overnight and transfected with the indicated vectors. At 24 h posttransfection, cells were washed three times with PBS and fixed by 4% paraformaldehyde. After having been permeated with 0.2% Triton X-100 for 15 min and three washes (each 5 min) with PBS, cells were incubated with the primary Abs against Flag and Myc overnight at 4°C, respectively. After another round of three washes with PBS, cells were incubated with the secondary Ab for 1 h at room temperature. Nuclei were stained by DAPI (10236276001; Roche). Intact cells were imaged using a FluoView 1000 confocal microscope (Olympus).

Statistical analysis

Statistical analysis was determined using the unpaired Student *t* test (comparison of two groups) or ANOVA (comparison of multiple groups) with Prism software (GraphPad). Unless otherwise noted, all results are representatives of at least three independent experiments, each with at least two biological replicates. Data were represented as mean ± SD.

Results

tGBP1 interacts with tSTING

We have previously reported that overexpression of tGBP1 inhibits VSV and HSV-1 replication in TSPRCs (29). In order to understand the mechanism of the antiviral function of tGBP1, we performed

coimmunoprecipitation screening to find out whether tGBP1 may interact with the immune factors tMDA5, tMAVS, and tSTING. *Tupaia* oligoadenylate synthetases-like 1 (tOASL1) was used as a positive control as it has been shown to interact with tMDA5, tMAVS, and tSTING in our previous study (45). tGBP1 specifically coimmunoprecipitated with tSTING but not with tMDA5 or tMAVS (Fig. 1A and 1B). HSV-1 infection did not affect the interaction between tGBP1 and tSTING (Fig. 1B). We also observed an interaction between endogenous tGBP1 and tSTING (Fig. 1C). However, tGBP1 did not interact with tSTING-mini, an alternative splicing variant of tSTING that was reported in our previous study (43) (Fig. 1D). tSTING-mini contained the first three TM domains and the incomplete fourth TM domain of tSTING, and is critical for RNA virus-induced antiviral signaling transduction (43). Consistent with coimmunoprecipitation results, the overexpressed tGBP1 was colocalized with tSTING in TSPRCs (Fig. 1E). These results collectively demonstrated that tGBP1 interacts with tSTING.

The CBD of tSTING mediates the interaction between tGBP1 and tSTING

tGBP1 contains a globular N-terminal GTPase domain and a CTD. As mentioned earlier, tSTING contains three domains: the TM domain, the CBD, and the CTT domain. We generated tGBP1 and tSTING truncated mutants to map the domain(s) of tGBP1 or of tSTING responsible for their interaction. Although both GTPase

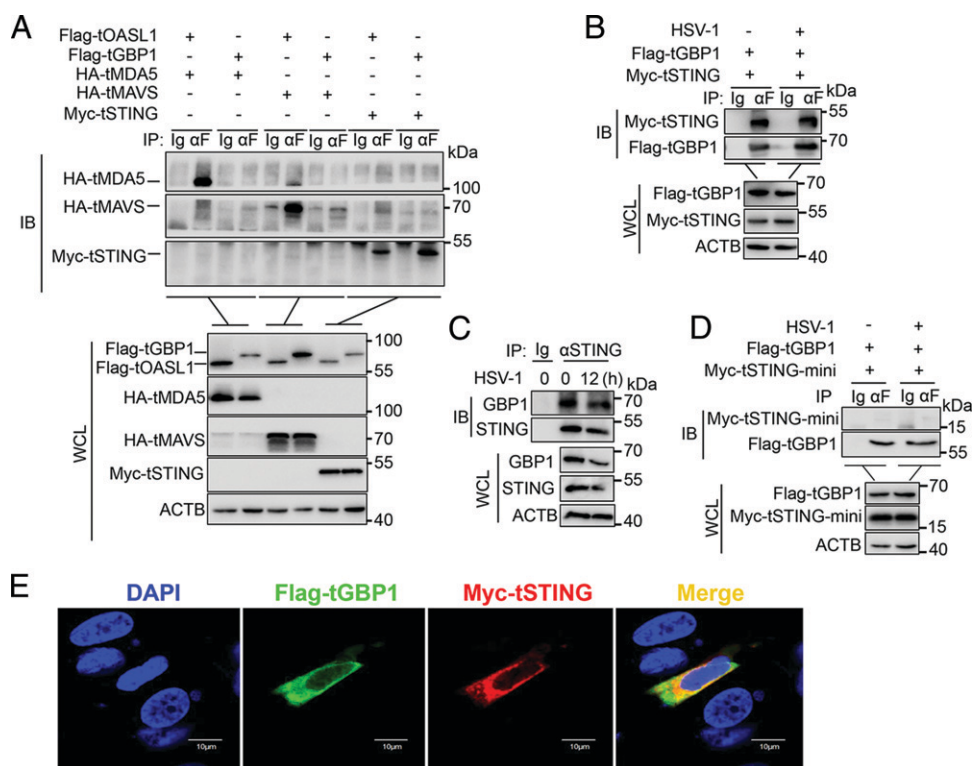


FIGURE 1. tGBP1 interacts with tSTING. **(A)** tGBP1 interacted with tSTING but not with tMDA5 or tMAVS. HEK293T cells were transfected with expression vector Flag-tGBP1, together with expression vector HA-tMDA5, HA-tMAVS, or Myc-tSTING. Expression vector Flag-tOASL1 was used as a positive control. Immunoprecipitation (IP, with anti-Flag) was performed at 24 h posttransfection and the immunoprecipitate was subjected to immunoblot (IB) analysis. **(B)** HSV-1 infection had no apparent effect on the interaction between tGBP1 and tSTING. HEK293T cells were cotransfected with expression vectors Flag-tGBP1 and Myc-tSTING, and infected with HSV-1 (MOI = 1) at 12 h posttransfection. IP (with anti-Flag) and IB were performed at 12 h postinfection to analyze the interaction between tGBP1 and tSTING. **(C)** Interaction between endogenous tGBP1 and tSTING. TSPRCs were infected with or without HSV-1 (MOI = 1) for 12 h. The interaction between endogenous tGBP1 and tSTING was analyzed by IP (with anti-STING) and IB. **(D)** No interaction between tGBP1 and tSTING-mini. HEK293T cells were cotransfected with expression vectors Flag-tGBP1 and Myc-tSTING-mini, then were infected with HSV-1 (MOI = 1) at 12 h posttransfection. IP and IB were performed at 12 h postinfection. **(E)** Colocalization of tGBP1 with tSTING in TSPRCs. Cells were cotransfected with expression vectors Flag-tGBP1 and Myc-tSTING for 24 h. The overexpressed tGBP1 and tSTING were immunostained by using anti-Flag (green) and anti-Myc (red). Nuclei were stained with DAPI (blue). Scale bar, 10 μm. The experiments were independently repeated three times with similar results. Shown results are a representative experiment. WCL, whole cell lysate.

domain and CTD of tGBP1 could interact with tSTING, the interaction between GTPase and tSTING was stronger than that between tGBP1 and tSTING, and deletion of GTPase domain (CTD) greatly hampered the interaction between tGBP1 and tSTING (Fig. 2A). These results indicated that the GTPase domain of tGBP1 plays a critical role in the interaction between tGBP1 and tSTING. The CBD of tSTING could interact with tGBP1, whereas deletion of the TM or CTT domain did not affect the interaction between tGBP1 and tSTING (Fig. 2B). These results indicated that the CBD of tSTING mediates the interaction between tSTING and tGBP1.

tGBP1 promotes autophagy in response to HSV-1 infection

In response to HSV-1 infection, STING induced IFN production and autophagy to restrict the viral replication (5, 7, 10, 39). As tGBP1 interacts with tSTING, we hypothesized that tGBP1 may play a role in the production of IFNs or autophagy in response to HSV-1 infection. However, overexpression of tGBP1 did not affect the mRNA expression of *tIFNβ1* and IFN-stimulated gene *tOAS1* in response to HSV-1 infection, whereas overexpression of tSTING significantly upregulated the mRNA expression levels of these two genes (Fig. 3A). We further examined the effect of tGBP1 overexpression on the IFN signaling induced by tSTING. Luciferase reporter assays showed that tGBP1 overexpression did not affect ISRE-Luc and NF-κB-Luc activation induced by tSTING (Fig. 3B). These results suggested that tGBP1 does not affect the IFN signaling induced by tSTING.

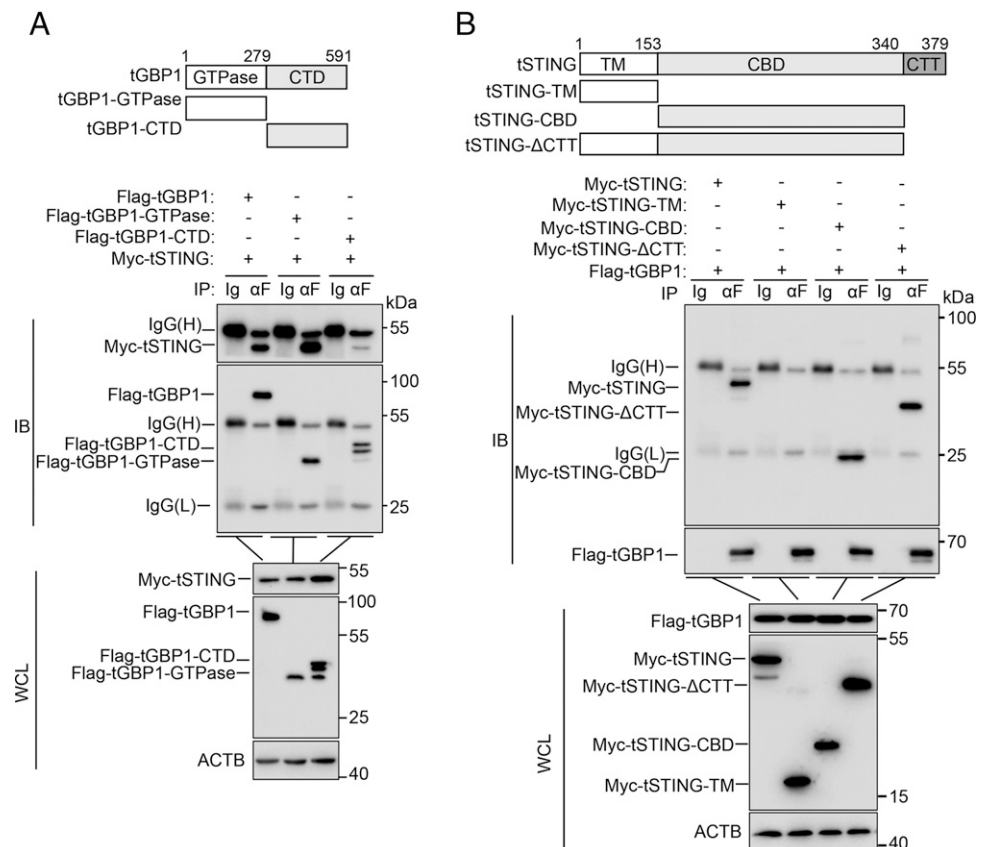
To explore the potential function of tGBP1 in autophagy induced by STING in response to HSV-1 infection, we firstly analyzed the tGBP1 expression pattern and autophagy upon HSV-1 infection. Compared with control, HSV-1 infection induced tGBP1 expression as early as 3 h in TSPRCs and TSR6 cells, and decreased it at 12 h (Supplemental Fig. 1). The autophagy was induced by HSV-1

infection at 6 h in TSPRCs and TSR6 cells, as manifested by the decreased SQSTM1 protein level and the increased ratio of LC3-II/LC3-I (Supplemental Fig. 1). In response to HSV-1 infection, tGBP1 overexpression decreased the SQSTM1 protein level but elevated the LC3-II:LC3-I ratio in TSPRCs (Fig. 3C, left panel), whereas no such effect on the changes of SQSTM1 and LC3-II:LC3-I was observed in TSR6-tGBP1-KO cells (Fig. 3C, right panel). The abolished effect on alterations of SQSTM1 and LC3-II:LC3-I ratio in TSR6-tGBP1-KO cells in response to HSV-1 infection could be rescued by overexpressing tGBP1 (Fig. 3D). These results clearly indicated that tGBP1 promotes autophagy in response to HSV-1 infection.

tGBP1 binds to tSTING, tSQSTM1, and tLC3

It has been reported that STING induced autophagy by a direct interaction with SQSTM1 and LC3 (9, 39) and GBPs targeted membranes via the LC3-conjugation system of autophagy (20). We speculated that tGBP1 may enhance autophagy by promoting the interaction between tSTING and tSQSTM1 or between tSTING and tLC3. However, overexpressed tSTING did not interact with either tSQSTM1 or tLC3, whereas the interaction between tSTING and tMDA5 described in our previous report (41) (as a positive control) could be well confirmed (Fig. 4A), suggesting that tSTING had a different strategy compared with human STING to interact with tSQSTM1 and tLC3 (9, 39). We next examined the interaction between tGBP1 and tSQSTM1 or tLC3. Coimmunoprecipitation assays showed that overexpressed tGBP1 interacts with tSQSTM1 and tLC3 (Fig. 4B). Note that an extra band with a small m.w. was detected for tGBP1 in the tSQSTM1 immunoprecipitate, along with the band with correct size. It may be the cleaved form of tGBP1 that should be secreted but was retained in the cytoplasm under certain conditions (47). Consistently, we could observe a colocalization

FIGURE 2. The CBD of tSTING is essential for the interaction between tGBP1 and tSTING. **(A)** Both GTPase domain and CTD of tGBP1 interacted with tSTING. HEK293T cells were transfected with expression vectors Myc-tSTING and Flag-tagged tGBP1 (Flag-tGBP1) or tGBP1 truncates (Flag-tGBP1-GTPase or Flag-tGBP1-CTD) for 24 h. Immunoprecipitation (IP, with anti-Flag) and immunoblot (IB) were performed to analyze the interaction between tSTING and tGBP1 or its truncates. **(B)** The CBD of tSTING mediated the interaction between tSTING and tGBP1. HEK293T cells were transfected with expression vectors Flag-tGBP1 and Myc-tSTING or tSTING truncates (Myc-tSTING-TM, Myc-tSTING-CBD, or Myc-tSTING-ΔCTT) for 24 h. IP (with anti-Flag) and IB were performed to show the interaction between tGBP1 and tSTING truncates. The experiments were independently repeated three times with similar results. Shown results are a representative experiment. WCL, whole cell lysate.



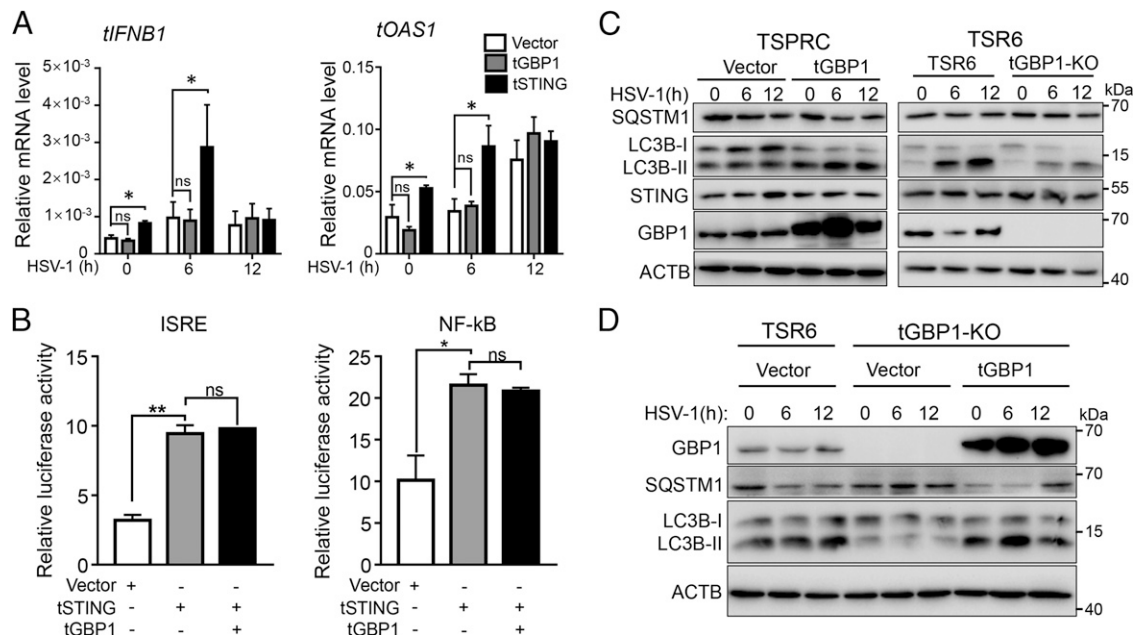


FIGURE 3. tGBP1 promotes autophagy in response to HSV-1 infection and this effect is independent on the IFN signaling. **(A)** tGBP1 did not affect type I IFN signaling in response to HSV-1 infection. TSPRCs were transiently transfected with pCMV-3Tag-8 (Vector, NC), pCMV-tGBP1-3Tag-8 (tGBP1), and pCMV-tSTING-3Tag-8 (tSTING, used as a positive control for upregulating *tIFNβ1* and *tOAS1* mRNA levels upon HSV-1 infection) for 12 h, then were infected with HSV-1 (MOI = 1) for the indicated times. The mRNA levels of *tIFNβ1* and *tOAS1* were analyzed by quantitative RT-PCR. **(B)** Overexpression of tGBP1 had no effect on ISRE-Luc and NF-κB-Luc reporter activation induced by tSTING. TSPRCs were cotransfected with the indicated expression vector (200 ng each), ISRE-Luc or NF-κB-Luc reporter vector (100 ng), and TK (10 ng, as an inner control) for 24 h before harvest for measuring the luciferase reporter activity. **(C)** tGBP1 promoted autophagy in response to HSV-1 infection. (Left panel) TSPRCs were transfected with empty vector or expression vector of tGBP1 for 24 h and were subjected to HSV-1 (MOI = 1) infection for the indicated times before the harvest for Western blotting. (Right panel) TSR6 cells and tGBP1-KO TSR6 cells were infected with HSV-1 (MOI = 1). The protein levels of SQSTM1, LC3B, STING, and ACTB (β -actin) were analyzed by Western blotting. **(D)** Re-overexpression of tGBP1 rescued autophagy in TSR6-tGBP1-KO cells induced by HSV-1 infection. Cells were seeded in 6-well plates and transfected with the indicated plasmids for 24 h followed by HSV-1 infection. The protein levels of GBP1, SQSTM1, LC3B, and ACTB were analyzed by Western blotting. The experiments were independently repeated three times with similar results. Each experiment in (A) and (B) had three biological repeats. Shown results are a representative experiment. Values are presented as mean \pm SD ($n = 3$ independent experiments). * $p < 0.05$, ** $p < 0.01$, two-way ANOVA. ns, not significant.

of overexpressed tGBP1 with overexpressed tSQSTM1 or tLC3 (Fig. 4C). Thus, tGBP1 might promote autophagy by mediating the interaction between tSTING and tSQSTM1 or tLC3. In accordance with this hypothesis, when tGBP1 and tSTING were overexpressed together with tSQSTM1 or tLC3, we could observe an interaction of tGBP1/tSTING/tSQSTM1 and of tGBP1/tSTING/tLC3 (Fig. 4D). These results indicated that tGBP1 binds to tSTING, tSQSTM1, and tLC3, and may function as a scaffold to promote autophagy in response to HSV-1 infection.

tGBP1 restricts HSV-1 production in TSR6

As tGBP1 interacts with tSTING and promotes autophagy in response to HSV-1 infection, we analyzed the effect of tGBP1 on HSV-1 infection by monitoring HSV-1-GFP production in TSR6 cells. Knockout of tGBP1 significantly promoted HSV-1-GFP production in TSR6 cells (Fig. 5A–C), whereas overexpression of tGBP1 in TSR6-tGBP1-KO cells significantly reversed the permissiveness of TSR6-tGBP1-KO cells for HSV-1-GFP production, and further inhibited HSV-1-GFP production in TSR6-tGBP1-KO cells (Fig. 5A–C). These results indicated that tGBP1 restricts HSV-1 production in TSR6 cells.

We next sought to determine whether tGBP1 restricts HSV-1 production via tSTING. Although overexpression of tGBP1 in TSR6 cells suppressed the production of HSV-1-GFP, this anti-HSV-1 effect of tGBP1 was lost in TSR6-tSTING-KO cells (Fig. 5D–F). To further confirm the essential role of tSTING for tGBP1 restricting HSV-1 production, we monitored the anti-HSV-1 activity of

tGBP1 in tSTING-rescued TSR6-tSTING-KO cells. Overexpression of tSTING into TSR6-tSTING-KO cells recovered anti-HSV-1 capability of tGBP1 (Fig. 5G–I). In addition, overexpression of tSTING- Δ CTT, a truncation of tSTING which possesses the ability to induce autophagy but lost the type I IFN inducing activity (10), also recovered anti-HSV-1 activity of tGBP1 in TSR6-tSTING-KO cells (Fig. 5G–I). These results indicated that anti-HSV-1 activity of tGBP1 is dependent on tSTING.

Discussion

cGAS and STING signalings play important roles in antiviral responses, as both are major cytoplasmic DNA sensors (11). cGAS detects viral infections or tissue damages by binding to microbial or self-DNA in the cytoplasm (4). Upon binding DNA, cGAS produces cGAMP that combines with and activates the adaptor protein STING (4, 6). STING then activates the production of IFNs to suppress viral infection. There are reports showing an IFN-independent antiviral activity of STING, in which STING mutant S365A devoid of the IFN signaling suppressed HSV-1 infection in mice (48) and STING- Δ CTT mutant (which lacks the CTT domain for the IFN signaling) could initiate autophagy to clear DNA and pathogens in the cytoplasm (7, 10). The mechanism and regulation of STING in activating IFNs has been extensively reported (49, 50), whereas the mechanism and regulation of STING in inducing autophagy are still insufficiently determined. In this study, we found that, in the Chinese tree shrew, tGBP1 directly binds to tSTING, tSQSTM1, and tLC3 to promote autophagy in response to HSV-1 infection. The

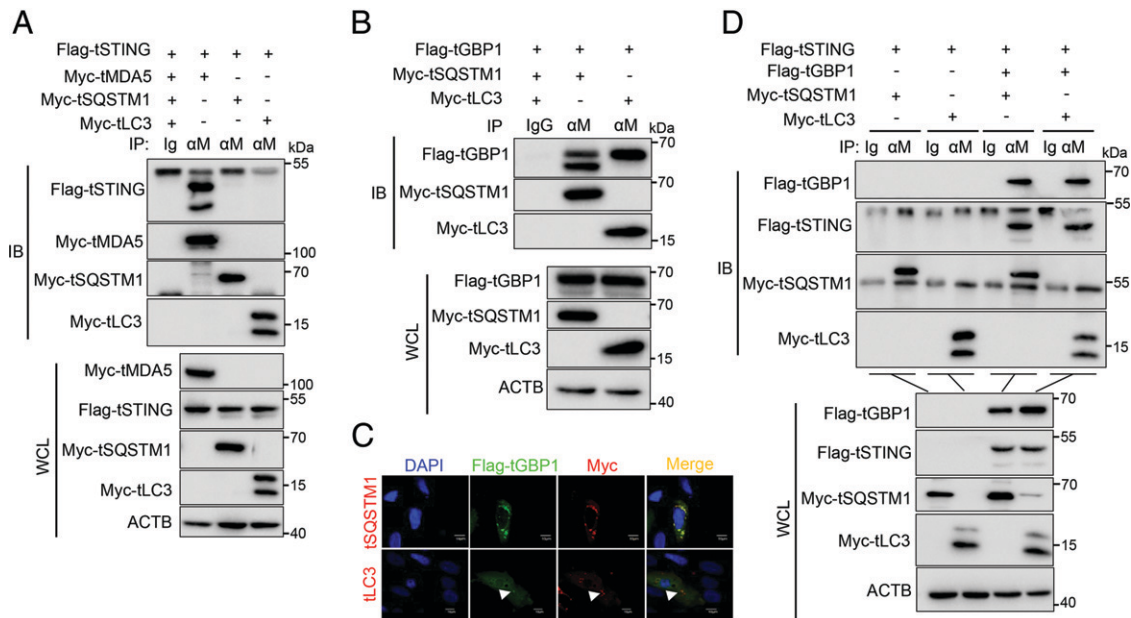


FIGURE 4. tGBP1 interacts with tSTING, tSQSTM1, and tLC3. **(A)** tSTING did not interact with tSQSTM1 or tLC3. HEK293T cells were cotransfected with expression vectors Flag-tSTING, Myc-tMDA5, Myc-tSQSTM1, and Myc-tLC3 for 24 h. The interactions between tSTING and tMDA5, SQSTM1, or tLC3 were analyzed by immunoprecipitation (IP, with anti-Myc) and immunoblot (IB). **(B)** tGBP1 interacted with tSQSTM1 and tLC3. HEK293T cells were transfected with expression vector Flag-tGBP1 together with expression vector Myc-tSQSTM1 or Myc-tLC3 for 24 h. The interactions between tGBP1 and SQSTM1 or tLC3 were analyzed by IP (with anti-Myc) and IB. **(C)** Colocalization of tGBP1 with tSQSTM1 and tLC3 in TSPRCs. Cells were cotransfected with expression vectors tGBP1-Flag and Myc-tSQSTM1 or tGBP1-Flag and tLC3 for 24 h. tGBP1, tSQSTM1, and tLC3 were immunostained by using anti-Flag (green) and anti-Myc (red). Nuclei were stained with DAPI (blue). Scale bar, 10 μ m. **(D)** tGBP1 combined with tSTING, tSQSTM1, and tLC3. HEK293T cells were cotransfected with expression vectors Flag-tSTING and Myc-tSQSTM1 or Myc-tLC3 with or without Flag-tGBP1 for 24 h. The interactions between tGBP1 and SQSTM1 or tLC3 were analyzed by IP (with anti-Myc) and IB. The experiments were independently repeated three times with similar results. Shown results are a representative experiment. WCL, whole cell lysate.

tGBP1 protein level was decreased at late stage of HSV-1 infection in TSPRCs and TSR6 cells (Supplemental Fig. 1), suggesting that HSV-1 infection may degrade tGBP1 and inhibits the endogenous interaction between tGBP1 and tSTING. More studies should be carried out to confirm this speculation. In humans, STING induces autophagy by directly interacting with SQSTM1 and LC3 (9, 10), which is different from that in the Chinese tree shrew. Specifically, we found that tGBP1 binds to tSTING and promotes autophagy, but the interaction between tGBP1 and tSTING does not affect *tIFN1* expression in response to HSV-1 infection, which may underlie the potential mechanism of the anti-HSV-1 activity of tGBP1. Consistent with this result, the anti-HSV-1 activity of tGBP1 was lost in TSR6-tSTING-KO cells, and overexpression of tSTING in TSR6-tSTING-KO cells rescued this anti-HSV-1 activity of tGBP1 (Fig. 5D–I). Furthermore, overexpression of tSTING- Δ CTT mutant, which possesses the ability to initiate autophagy but has no type I IFN induction activity (10), also rescued the anti-HSV-1 activity of tGBP1. These findings demonstrated that tGBP1 restricts HSV-1 infection by interacting with tSTING and promoting autophagy. Previously, GBP1 has been reported to restrict infection of a variety of viruses, such as VSV (24, 25), encephalomyocarditis virus (24), hepatitis C virus (26), classical swine fever virus (28), and KSHV (27); our findings further broaden the antiviral spectrum and mechanism of GBP1.

The host defense function of GBPs was tightly related to autophagy. For example, mouse GBP1 binds to SQSTM1 and GBP7 interacts with ATG4B, respectively, to deliver bacteria to larger LC3B marked vacuoles for liberating mycobactericidal peptides (18). Human GBP1 and GBP2 mediate the restriction of *Chlamydia trachomatis* growth by autophagy in human macrophages (19). Most recently, it was reported that GBPs target the replication complexes

of murine norovirus via the LC3 conjugation system necessary for inhibiting murine norovirus replication in mice and human cells (51). Our result provides an additional line of evidence that GBP1 controls viral infection via autophagy, albeit the difference between human and tree shrew.

The interaction between STING and GBP1 may be involved in other physiological processes. Firstly, GBPs bind to and lyse cytosolic bacteria, prompting the spillage of bacterial DNA into the host cell cytosol (17, 52). The interaction of GBP1 and STING may recruit STING to the site of the infection, promoting the sensing of bacterial DNA and c-di-GMP by STING (5) and thereby inducing the production of IFNs and autophagy (7, 39). Secondly, GBP1 functions as a negative regulator of T cell activation (53). A recent study showed that activation of STING leads to T cell death in an IFN-independent manner (54). Whether this process is associated with the interaction between tGBP1 and tSTING is also worthy of further study.

The current study has some limitations. Firstly, most of these cellular assays are conducted in the context of exogenous overexpression of tagged proteins. Secondly, we did not obtain living cellular data to show the colocalization and formation of STING/LC3/GBP1 punctae in response to viral infection in the tree shrew cells. Thirdly, although we had previously determined the characteristics of tSTING (43), whether the interaction between tSTING and tGBP1 would have an impact on balancing activation of IFN regulatory factor 3–dependent and NF- κ B-dependent transcriptions (55) remains to be further determined.

In short, we found that tGBP1 has a moderate antiviral activity against HSV-1 in a tSTING-dependent manner. The interaction between tGBP1 and tSTING did not affect IFN signaling but promoted autophagy via interaction among tGBP1, tSTING, tSQSTM1,

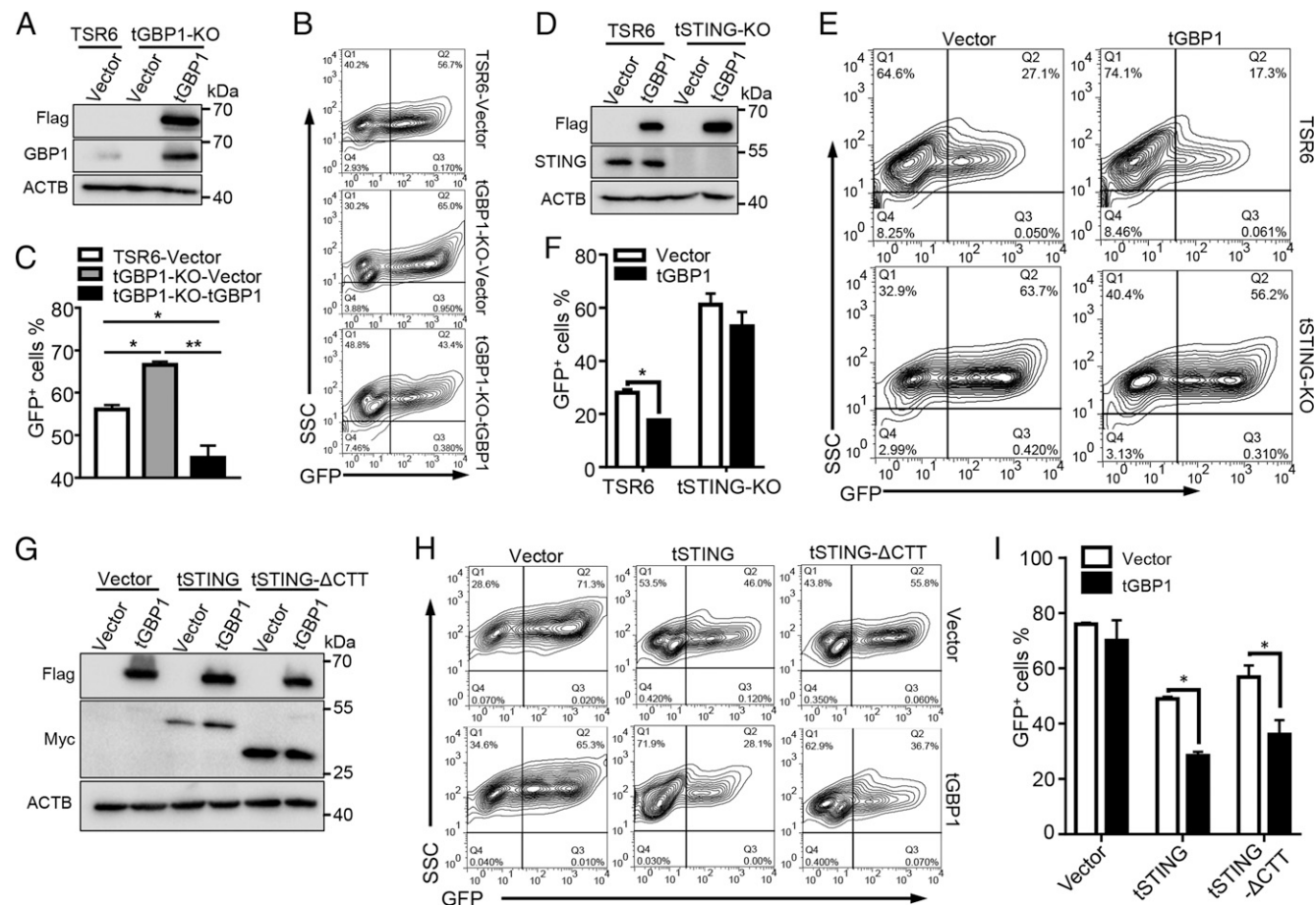


FIGURE 5. tGBP1 restricts HSV-1 replication and this anti-HSV-1 activity is dependent on tSTING. **(A–C)** Knockout of tGBP1 enhanced HSV-1 replication. **(A)** Successful knockout and rescue of tGBP1 in TSR6 cells with tGBP1 knockout (tGBP1-KO) and wild-type TSR6 cells that were transfected with empty vector (Vector) or expression vector Flag-tGBP1 (tGBP1). **(B)** Flow cytometry analyses for TSR6 and tGBP1-KO cells transfected with empty vector (TSR6-Vector and tGBP1-KO-Vector) or Flag-tGBP1 (tGBP1-KO-tGBP1) after 48 h infection with HSV-1-GFP (MOI = 1). The production of HSV-1-GFP was quantified by detecting the GFP expression, and **(C)** percentage of 10,000 cells expressing GFP (GFP⁺ cells) were counted. **(D–F)** The anti-HSV-1 activity of tGBP1 was dependent on tSTING. **(D)** Successful overexpression or knockout of tGBP1 in TSR6 cells with tSTING knockout (tSTING-KO) and wild-type TSR6 cells that were transfected with empty vector (Vector) or Flag-tGBP1 (tGBP1). **(E)** Flow cytometry analyses for cells in **(D)** after HSV-1-GFP (MOI = 1) infection for 48 h, and production of HSV-1-GFP was quantified by counting **(F)** the percentage of 10,000 cells expressing GFP (GFP⁺ cells). **(G)** Successful overexpression of expression vectors Myc-tSTING (tSTING) and Myc-tSTING-ΔCTT (tSTING-ΔCTT) in TSR6 cells with tSTING knockout, and with transfection of Flag-tGBP1 (tGBP1) or empty vector (Vector). Transfected cells were infected by HSV-1-GFP (MOI = 1) for 48 h before the harvest for Western blotting. **(H and I)** Production of HSV-1-GFP in cells in **(G)** was quantified by GFP expression using flow cytometry. Experiments were independently repeated three times with similar results. Each experiment had two biological repeats. Shown results are a representative experiment. Values are presented as mean ± SD (*n* = 3 independent experiments). **p* < 0.05, ***p* < 0.01, one-way ANOVA for **(C)** and two-tailed unpaired Student *t* test for **(F and I)**.

and tLC3. These results suggested a tGBP1-dependent increase in tSTING-mediated autophagy in response to HSV-1 infection.

Acknowledgments

We thank Dr. Ian Logan for language editing, Drs. Ling-Yan Su and Qianjin Liu for critical discussions, and Guolan Ma and Cong Li (Public Technology Service Center, Kunming Institute of Zoology, Chinese Academy of Sciences) for technical support in flow cytometric analyses.

Disclosures

The authors declare that they have no conflicts of interest.

References

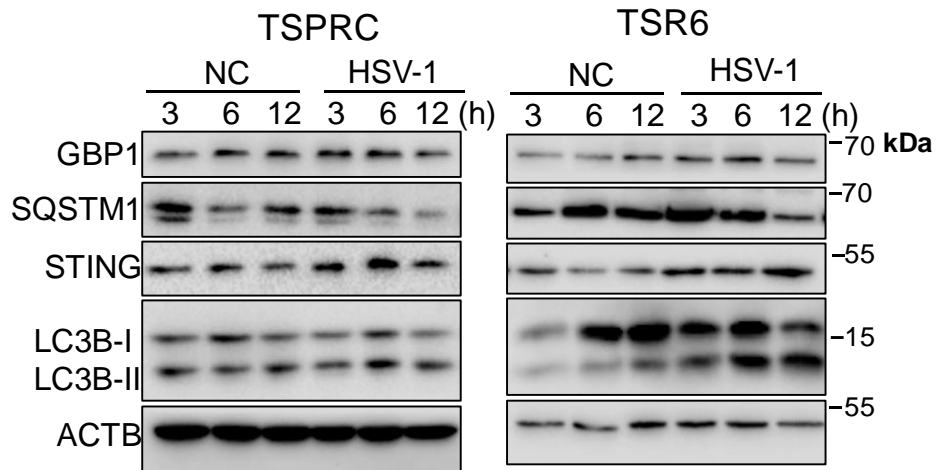
- McNab, F., K. Mayer-Barber, A. Sher, A. Wack, and A. O’Garra. 2015. Type I interferons in infectious disease. *Nat. Rev. Immunol.* 15: 87–103.
- Akira, S., S. Uematsu, and O. Takeuchi. 2006. Pathogen recognition and innate immunity. *Cell* 124: 783–801.
- Takeuchi, O., and S. Akira. 2010. Pattern recognition receptors and inflammation. *Cell* 140: 805–820.
- Sun, L., J. Wu, F. Du, X. Chen, and Z. J. Chen. 2013. Cyclic GMP-AMP synthase is a cytosolic DNA sensor that activates the type I interferon pathway. *Science* 339: 786–791.
- Burdette, D. L., K. M. Monroe, K. Sotelo-Troha, J. S. Iwig, B. Eckert, M. Hyodo, Y. Hayakawa, and R. E. Vance. 2011. STING is a direct innate immune sensor of cyclic di-GMP. *Nature* 478: 515–518.
- Wu, J., L. Sun, X. Chen, F. Du, H. Shi, C. Chen, and Z. J. Chen. 2013. Cyclic GMP-AMP is an endogenous second messenger in innate immune signaling by cytosolic DNA. *Science* 339: 826–830.
- Ishikawa, H., Z. Ma, and G. N. Barber. 2009. STING regulates intracellular DNA-mediated, type I interferon-dependent innate immunity. *Nature* 461: 788–792.
- Zhao, B., F. Du, P. Xu, C. Shu, B. Sankaran, S. L. Bell, M. Liu, Y. Lei, X. Gao, X. Fu, et al. 2019. A conserved PLPLRT/SD motif of STING mediates the recruitment and activation of TBK1. *Nature* 569: 718–722.
- Prabakaran, T., C. Bodda, C. Krapp, B. C. Zhang, M. H. Christensen, C. Sun, L. Reinert, Y. Cai, S. B. Jensen, M. K. Skouboe, et al. 2018. Attenuation of cGAS-STING signaling is mediated by a p62/SQSTM1-dependent autophagy pathway activated by TBK1. *EMBO J.* 37: e97858.
- Gui, X., H. Yang, T. Li, X. Tan, P. Shi, M. Li, F. Du, and Z. J. Chen. 2019. Autophagy induction via STING trafficking is a primordial function of the cGAS pathway. *Nature* 567: 262–266.

11. Hopfner, K. P., and V. Hornung. 2020. Molecular mechanisms and cellular functions of cGAS-STING signalling. *Nat. Rev. Mol. Cell Biol.* 21: 501–521.
12. Olszewski, M. A., J. Gray, and D. J. Vestal. 2006. *In silico* genomic analysis of the human and murine guanylate-binding protein (GBP) gene clusters. *J. Interferon Cytokine Res.* 26: 328–352.
13. Degrandi, D., C. Konermann, C. Beuter-Gunia, A. Kresse, J. Würthner, S. Kurig, S. Beer, and K. Pfeffer. 2007. Extensive characterization of IFN-induced GTPases mGBP1 to mGBP10 involved in host defense. *J. Immunol.* 179: 7729–7740.
14. Tretina, K., E.-S. Park, A. Maminska, and J. D. MacMicking. 2019. Interferon-induced guanylate-binding proteins: guardians of host defense in health and disease. *J. Exp. Med.* 216: 482–500.
15. Lubeseder-Martellato, C., E. Guenzi, A. Jörg, K. Töpolt, E. Naschberger, E. Kremmer, C. Zietz, E. Tschachler, P. Hutzler, M. Schwemmler, et al. 2002. Guanylate-binding protein-1 expression is selectively induced by inflammatory cytokines and is an activation marker of endothelial cells during inflammatory diseases. *Am. J. Pathol.* 161: 1749–1759.
16. Kutsch, M., and J. Coers. 2020. Human guanylate binding proteins: nanomachines orchestrating host defense. *FEBS J.* DOI: 10.1111/febs.15662.
17. Pilla-Moffett, D., M. F. Barber, G. A. Taylor, and J. Coers. 2016. Interferon-inducible GTPases in host resistance, inflammation and disease. *J. Mol. Biol.* 428: 3495–3513.
18. Kim, B. H., A. R. Shenoy, P. Kumar, R. Das, S. Tiwari, and J. D. MacMicking. 2011. A family of IFN- γ -inducible 65-kD GTPases protects against bacterial infection. *Science* 332: 717–721.
19. Al-Zeer, M. A., H. M. Al-Younes, D. Lauster, M. Abu Lubad, and T. F. Meyer. 2013. Autophagy restricts *Chlamydia trachomatis* growth in human macrophages via IFN γ -inducible guanylate binding proteins. *Autophagy* 9: 50–62.
20. Choi, J., S. B. Biering, and S. Hwang. 2017. Quo vadis? Interferon-inducible GTPases go to their target membranes via the LC3-conjugation system of autophagy. *Small GTPases* 8: 199–207.
21. Choi, J., S. Park, S. B. Biering, E. Selleck, C. Y. Liu, X. Zhang, N. Fujita, T. Saitoh, S. Akira, T. Yoshimori, et al. 2014. The parasitophorous vacuole membrane of *Toxoplasma gondii* is targeted for disruption by ubiquitin-like conjugation systems of autophagy. *Immunity* 40: 924–935.
22. Haldar, A. K., C. Foltz, R. Finethy, A. S. Piro, E. M. Feeley, D. M. Pilla-Moffett, M. Komatsu, E. M. Frickel, and J. Coers. 2015. Ubiquitin systems mark pathogen-containing vacuoles as targets for host defense by guanylate binding proteins. *Proc. Natl. Acad. Sci. USA* 112: E5628–E5637.
23. Santos, J. C., D. Boucher, L. K. Schneider, B. Demarco, M. Dilucca, K. Shkarina, R. Heilig, K. W. Chen, R. Y. H. Lim, and P. Broz. 2020. Human GBP1 binds LPS to initiate assembly of a caspase-4 activating platform on cytosolic bacteria. *Nat. Commun.* 11: 3276.
24. Anderson, S. L., J. M. Carton, J. Lou, L. Xing, and B. Y. Rubin. 1999. Interferon-induced guanylate binding protein-1 (GBP-1) mediates an antiviral effect against vesicular stomatitis virus and encephalomyocarditis virus. *Virology* 256: 8–14.
25. Gu, T., D. Yu, L. Xu, Y. L. Yao, X. Zheng, and Y. G. Yao. 2021. *Tupaia* guanylate-binding protein 1 interacts with vesicular stomatitis virus phosphoprotein and represses primary transcription of the viral genome. *Cytokine* 138: 155388.
26. Itsui, Y., N. Sakamoto, S. Kakinuma, M. Nakagawa, Y. Sekine-Osajima, M. Tasaka-Fujita, Y. Nishimura-Sakurai, G. Suda, Y. Karakama, K. Mishima, et al. 2009. Antiviral effects of the interferon-induced protein guanylate binding protein 1 and its interaction with the hepatitis C virus NS5B protein. *Hepatology* 50: 1727–1737.
27. Zou, Z., Z. Meng, C. Ma, D. Liang, R. Sun, and K. Lan. 2017. Guanylate-binding protein 1 inhibits nuclear delivery of Kaposi's sarcoma-associated herpesvirus virions by disrupting formation of actin filament. *J. Virol.* 91: e00632-17.
28. Li, L. F., J. Yu, Y. Li, J. Wang, S. Li, L. Zhang, S. L. Xia, Q. Yang, X. Wang, S. Yu, et al. 2016. Guanylate-binding protein 1, an interferon-induced GTPase, exerts an antiviral activity against classical swine fever virus depending on its GTPase activity. *J. Virol.* 90: 4412–4426.
29. Gu, T., D. Yu, Y. Fan, Y. Wu, Y. L. Yao, L. Xu, and Y. G. Yao. 2019. Molecular identification and antiviral function of the guanylate-binding protein (GBP) genes in the Chinese tree shrew (*Tupaia belangeri chinensis*). *Dev. Comp. Immunol.* 96: 27–36.
30. Fan, Y., Z. Y. Huang, C. C. Cao, C. S. Chen, Y. X. Chen, D. D. Fan, J. He, H. L. Hou, L. Hu, X. T. Hu, et al. 2013. Genome of the Chinese tree shrew. *Nat. Commun.* 4: 1426.
31. Fan, Y., M. S. Ye, J. Y. Zhang, L. Xu, D. D. Yu, T. L. Gu, Y. L. Yao, J. Q. Chen, L. B. Lv, P. Zheng, et al. 2019. Chromosomal level assembly and population sequencing of the Chinese tree shrew genome. *Zool. Res.* 40: 506–521.
32. Xu, S., X. Li, J. Yang, Z. Wang, Y. Jia, L. Han, L. Wang, and Q. Zhu. 2019. Comparative pathogenicity and transmissibility of pandemic H1N1, avian H5N1, and human H7N9 influenza viruses in tree shrews. *Front. Microbiol.* 10: 2955.
33. Xiao, J., R. Liu, and C. S. Chen. 2017. Tree shrew (*Tupaia belangeri*) as a novel laboratory disease animal model. *Zool. Res.* 38: 127–137.
34. Yao, Y. G. 2017. Creating animal models, why not use the Chinese tree shrew (*Tupaia belangeri chinensis*)? *Zool. Res.* 38: 118–126.
35. Amako, Y., K. Tsukiyama-Kohara, A. Katsume, Y. Hirata, S. Sekiguchi, Y. Tobita, Y. Hayashi, T. Hishima, N. Funata, H. Yonekawa, and M. Kohara. 2010. Pathogenesis of hepatitis C virus infection in *Tupaia belangeri*. *J. Virol.* 84: 303–311.
36. Li, L., Z. Li, E. Wang, R. Yang, Y. Xiao, H. Han, F. Lang, X. Li, Y. Xia, F. Gao, et al. 2016. Herpes simplex virus 1 infection of tree shrews differs from that of mice in the severity of acute infection and viral transcription in the peripheral nervous system. *J. Virol.* 90: 790–804.
37. Zhang, J., R. C. Luo, X. Y. Man, L. B. Lv, Y. G. Yao, and M. Zheng. 2020. The anatomy of the skin of the Chinese tree shrew is very similar to that of human skin. *Zool. Res.* 41: 208–212.
38. Ni, R. J., Y. Tian, X. Y. Dai, L. S. Zhao, J. X. Wei, J. N. Zhou, X. H. Ma, and T. Li. 2020. Social avoidance behavior in male tree shrews and prosocial behavior in male mice toward unfamiliar conspecifics in the laboratory. *Zool. Res.* 41: 258–272.
39. Liu, D., H. Wu, C. Wang, Y. Li, H. Tian, S. Siraj, S. A. Sehgal, X. Wang, J. Wang, Y. Shang, et al. 2019. STING directly activates autophagy to tune the innate immune response. *Cell Death Differ.* 26: 1735–1749.
40. Yu, D., L. Xu, X. H. Liu, Y. Fan, L. B. Lü, and Y. G. Yao. 2014. Diverse interleukin-7 mRNA transcripts in Chinese tree shrew (*Tupaia belangeri chinensis*). *PLoS One* 9: e99859.
41. Xu, L., D. Yu, Y. Fan, L. Peng, Y. Wu, and Y. G. Yao. 2016. Loss of RIG-I leads to a functional replacement with MDA5 in the Chinese tree shrew. *Proc. Natl. Acad. Sci. USA* 113: 10950–10955.
42. Gu, T., D. Yu, Y. Li, L. Xu, Y. L. Yao, and Y. G. Yao. 2019. Establishment and characterization of an immortalized renal cell line of the Chinese tree shrew (*Tupaia belangeri chinensis*). *Appl. Microbiol. Biotechnol.* 103: 2171–2180.
43. Xu, L., D. Yu, L. Peng, Y. Wu, Y. Fan, T. Gu, Y. L. Yao, J. Zhong, X. Chen, and Y. G. Yao. 2020. An alternative splicing of *Tupaia* STING modulated anti-RNA virus responses by targeting MDA5-LGP2 and IRF3. *J. Immunol.* 204: 3191–3204.
44. Ran, F. A., P. D. Hsu, J. Wright, V. Agarwala, D. A. Scott, and F. Zhang. 2013. Genome engineering using the CRISPR-Cas9 system. *Nat. Protoc.* 8: 2281–2308.
45. Yao, Y. L., D. Yu, L. Xu, T. Gu, Y. Li, X. Zheng, R. Bi, and Y. G. Yao. 2020. *Tupaia* OASL1 promotes cellular antiviral immune responses by recruiting MDA5 to MAVS. *J. Immunol.* 205: 3419–3428.
46. Yu, D., Y. Wu, L. Xu, Y. Fan, L. Peng, M. Xu, and Y. G. Yao. 2016. Identification and characterization of toll-like receptors (TLRs) in the Chinese tree shrew (*Tupaia belangeri chinensis*). *Dev. Comp. Immunol.* 60: 127–138.
47. Naschberger, E., W. Geißdörfer, C. Bogdan, P. Tripal, E. Kremmer, M. Stürzl, and N. Britzen-Laurent. 2017. Processing and secretion of guanylate binding protein-1 depend on inflammatory caspase activity. *J. Cell. Mol. Med.* 21: 1954–1966.
48. Yamashiro, L. H., S. C. Wilson, H. M. Morrison, V. Karalis, J. J. Chung, K. J. Chen, H. S. Bateup, M. L. Szpara, A. Y. Lee, J. S. Cox, and R. E. Vance. 2020. Interferon-independent STING signaling promotes resistance to HSV-1 in vivo. *Nat. Commun.* 11: 3382.
49. Chen, Q., L. Sun, and Z. J. Chen. 2016. Regulation and function of the cGAS-STING pathway of cytosolic DNA sensing. *Nat. Immunol.* 17: 1142–1149.
50. Gallucci, S., and M. E. Maffei. 2017. DNA sensing across the tree of life. *Trends Immunol.* 38: 719–732.
51. Biering, S. B., J. Choi, R. A. Halstrom, H. M. Brown, W. L. Beatty, S. Lee, B. T. McCune, E. Dominici, L. E. Williams, R. C. Orchard, et al. 2017. Viral replication complexes are targeted by LC3-guided interferon-inducible GTPases. *Cell Host Microbe* 22: 74–85.e7.
52. Meunier, E., P. Wallet, R. F. Dreier, S. Costanzo, L. Anton, S. Rühl, S. Dussurgey, M. S. Dick, A. Kistner, M. Rigard, et al. 2015. Guanylate-binding proteins promote activation of the AIM2 inflammasome during infection with *Francisella novicida*. *Nat. Immunol.* 16: 476–484.
53. Forster, F., W. Paster, V. Supper, P. Schatzlmaier, S. Sunzenauer, N. Ostler, A. Saliba, P. Eckerstorfer, N. Britzen-Laurent, G. Schütz, et al. 2014. Guanylate binding protein 1-mediated interaction of T cell antigen receptor signaling with the cytoskeleton. *J. Immunol.* 192: 771–781.
54. Wu, J., N. Dobbs, K. Yang, and N. Yan. 2020. Interferon-independent activities of mammalian STING mediate antiviral response and tumor immune evasion. *Immunity* 53: 115–126.e5.
55. de Oliveira Mann, C. C., M. H. Orzalli, D. S. King, J. C. Kagan, A. S. Y. Lee, and P. J. Kranzusch. 2019. Modular architecture of the STING C-terminal tail allows interferon and NF- κ B signaling adaptation. *Cell Rep.* 27: 1165–1175.e5.

Table S1 Primers used in this study

Gene	Name	Primer sequence (5' - 3')	Application
<i>tGBP1</i>	tGBP1-GTPase F	ATGCGGATCCATGGCCTCAGAGAACCACAT	PCR for constructing pCMV-tGBP1-GTPase-3Tag-8 using pCMV-3Tag-8 vector
	tGBP1-GTPase R	ATGCCTCGAGAAGAGTTTTAACCTTGGCA	
	tGBP1-CTD F	ATGCGGATCCATGTCAGGAGGCATCAAGA	PCR for constructing pCMV-tGBP1-CTD-3Tag-8 using pCMV-3Tag-8 vector
	tGBP1-CTD R	ATGCCTCGAGACTTATGACACATGTCTTCTTTGGC	
<i>tSQSTM1</i>	myc-tSQSTM1 F	tccggaagatctgagctcgagATGGCGTCGCTCACGGTG	PCR for constructing pCS2-N-myc-tSQSTM1 using pCS2-N-myc vector
	myc-tSQSTM1 R	ctatagttctagaggctcgagTCACAAGGGCGGGGGGTG	
<i>tLC3B</i>	myc-tLC3B F	tccggaagatctgagctcgagATGCCGTCGGAGAAGACCTT	PCR for constructing pCS2-N-myc-tLC3B using pCS2-N-myc vector
	myc-tLC3B R	ctatagttctagaggctcgagTTACTGACGGTTTCCTTCCAA	
<i>tSTING</i>	tSTING-3Tag-8 F	agetccaccgcggtggcgccgcATGCCCCACTCCAGCCTG	PCR for constructing pCMV-tSTING-3Tag-8 using pCMV-3Tag-8 vector
	tSTING-3Tag-8 R	gtcatccttgaatcctcgagTCAGAAGACATCCGTGCGGA	
	myc-tSTING-TM F	ccggaagatctgagctcgagATGCCCCACTCCAGCCTGCAT	PCR for constructing pCS2-N-myc-tSTING-TM using pCS2-N-myc vector
	myc-tSTING-TM R	tatagttctagaggctcgagCTAGAAGTTCCCTTTGTTACAG	
	myc-tSTING-CBD F	ccggaagatctgagctcgagATGAATGTGGCCACGGCTT	PCR for constructing pCS2-N-myc-tSTING-CBD using pCS2-N-myc vector
	myc-tSTING-CBD R	tatagttctagaggctcgagTCACTCTTCCTTTTCCTCCTGC	
<i>tOAS1</i>	myc-tSTING- Δ CTT F	ccggaagatctgagctcgagATGCCCCACTCCAGCCTGCAT	PCR for constructing pCS2-N-myc-tSTING- Δ CTT using pCS2-N-myc vector
	myc-tSTING- Δ CTT R	tatagttctagaggctcgagTCACTCTTCCTTTTCCTCCTGC	
<i>tOAS1</i>	tOAS1 F	CATCAACATCATTTCCGATT	Analytical qRT-PCR for <i>tOAS1</i>
	tOAS1 R	CTTACCACCTTCACTAC	
<i>tIFN1</i>	tIFN1 F	ACCACTTGGAACCATGC	Analytical qRT-PCR for <i>tIFN1</i>
	tIFN1 R	TTTCCACTCGGACTATCG	
<i>tβ-actin</i>	t β -actin F	ATTTTGAATGATCAGCCACC	Analytical qRT-PCR for <i>tβ-actin</i>
	t β -actin R	AGGTAAGCCCTGGCTGCCTC	

Notes: The nucleotides in italic stand for the site of restriction enzyme, and the nucleotides in the lowercase stand for homologous sequence. qRT-PCR, quantitative real-time PCR



Supplementary Figure 1. HSV-1 infection induced tGBP1 protein expression and affected autophagy in TSPRCs and TSR6 cells. Cells were seeded in 6-well plates and were infected with or without HSV-1 (MOI=1) for indicated times before harvest. The protein levels of tGBP1, tSQSTM1, tLC3B, tSTING and ACTB (β -actin, as a loading control) were analyzed by Western blotting. The experiments were independently repeated three times with similar results. Shown result is a representative experiment. NC, uninfected control.